

Study of Microstructure and Texture of Hot-deformed TXA321 Magnesium Alloy

*C. Dharmendra¹⁾, K.P. Rao²⁾, Y.V.R.K. Prasad³⁾, N. Hort⁴⁾ and K.U. Kainer⁵⁾

¹⁾²⁾ *Department of Mechanical and Biomedical Engineering, City University of Hong Kong, 81 Tat Chee Avenue, Kowloon, Hong Kong SAR, China*

³⁾ *processingmaps.com (formerly at City University of Hong Kong, Hong Kong, China)*

⁴⁾⁵⁾ *Helmoltz-Zentrum Geesthacht, Max-Planck Str. 1, Geesthacht 21502, Germany*

¹⁾ dchalan2@student.cityu.edu.hk

ABSTRACT

The influence of temperature and strain rate on the flow behavior and microstructure were examined in order to determine formability characteristics of Mg-3Sn-2Ca-1Al (TXA321) alloy. Uniaxial compression tests were carried out at elevated temperatures with different strain rates. The microstructural characterization was carried out using optical microscopy and electron backscattered diffraction (EBSD). The stress-strain responses strongly depend on the temperature. The processing map exhibits four dynamic recrystallization (DRX) domains occurring at discrete temperature and strain rate ranges and the alloy can be successfully hot worked over two of these domains. The basal pole distribution is almost parallel to the compression axis at lower temperatures (300 °C and 350 °C) and strain rates (0.0003 s⁻¹, 0.001 s⁻¹). With increase in temperature and strain rate, basal poles tilted away from the compression axis indicating enhanced basal slip activity. The results showed that fully recrystallized structures evolved with increase in temperature and non-basal slip activity.

¹⁾ Graduate Student

²⁾ Associate Professor

³⁾ Consultant

⁴⁾ Head, Magnesium processing group

⁵⁾ Director, Magnesium Innovation Centre

1. INTRODUCTION

Wrought magnesium alloys are receiving high attention in automotive industries (as structural materials) and electronics materials. Mg-Al series alloys are being widely used magnesium alloys at present, such as AM60 and AZ91 alloys, but insufficient strength and corrosion resistance at elevated temperatures limiting their structural applications. In recent years, Mg-Sn-Ca (TX) series alloys are being developed with a view to improve the corrosion and creep resistance (Abu Leil 2006, 2007). In this series alloys, (i) Sn can impart corrosion resistance; (ii) Ca forms the stable Mg_2Ca compound; (iii) Sn and Ca together with Mg forms the stable intermetallic compound $CaMgSn$. From the recent studies, Mg-3Sn-2Ca (wt%) alloy has been identified as one of the promising Mg-Sn-Ca alloys (Rao 2007, Kozlov 2008). To strengthen the alloy further, aluminum addition is considered as it can cause solid solution strengthening of magnesium.

Magnesium develops strong textures during processing (Hosford 1993) but the alloying additions can alter the deformation modes which in turn influence texture characteristics. The objective of the present work is to characterize the hot compressive deformation behavior of as-cast Mg-3Sn-2Ca-1Al (TXA321) alloy by using the processing map technique and to study the microstructure and texture development under various deformation conditions. Processing maps can be developed based on the Dynamic Materials Model (Prasad 1984), the principles of which were described in earlier publications (Prasad 1998, 2003).

2. EXPERIMENTAL WORK

Mg-3 wt.% Sn-2 wt.% Ca-1wt.% Al (TXA321) alloy was prepared using 99.99% pure Mg, 99.96% pure Sn, 98.5% pure Ca and 99.9% pure Al. The alloy, molten at about 720 °C, was kept under a protective cover of Ar+3% SF_6 gas before casting in a pre-heated permanent mold (200 °C) to obtain cylindrical billets of 100 mm diameter and 350 mm length.

Cylindrical specimens of 10 mm diameter and 15 mm height were machined from the as-cast billet for compression testing. A thermocouple is inserted at mid-height of the specimen to measure the temperature as well as the adiabatic temperature rise during deformation. The data for developing processing maps were obtained in isothermal uniaxial compression tests that were conducted at constant true strain rates in the range $0.0003 - 10 \text{ s}^{-1}$ and temperature range 300 – 500 °C. Details of the test set-up and procedure are described in an earlier publication [Prasad 2008]. The load – stroke data were converted into true stress - true strain curves using standard equations. The flow stress values were corrected for the adiabatic temperature rise at different temperatures and strain rates.

The deformed specimens were sectioned in the center parallel to the compression axis and the cut surface was mounted, polished and etched for microstructure examination by optical microscopy. The texture of the deformed samples for selected deformed conditions was examined using a JEOL 5600 SEM equipped with a NordlysF EBSD detector and HKL Channel 5 software was used for data collection. Output texture data is shown as pole figures (compression axis is horizontal).

3. RESULTS AND DISCUSSION

3.1 Initial As-cast Microstructure

The microstructure of the starting material (TXA321) in cast condition is shown in Fig. 1(a) which exhibits large grains of about 300 μm diameter. The microstructure revealed the presence of intermetallic particles: CaMgSn mainly distributed within the matrix and Mg_2Ca preferentially formed at the grain boundaries, as marked on the SEM image in Fig. 1(b).

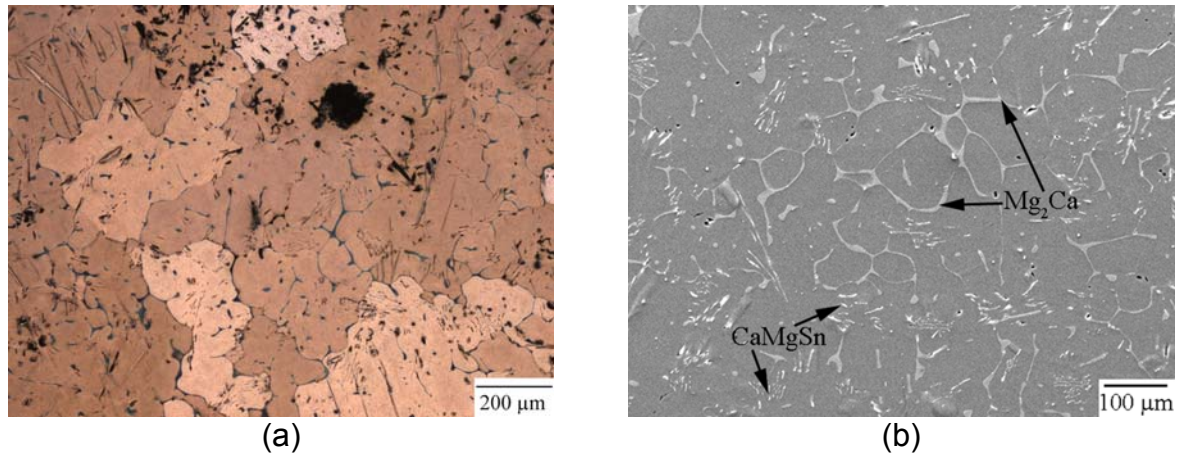


Fig. 1. Initial microstructure of TXA321 magnesium alloy in as-cast condition: (a) Optical micrograph, (b) SEM image with phases marked.

3.2 Compressive Stress-strain Behavior

The true stress - true strain curves obtained under isothermal compression tests at 450 $^{\circ}\text{C}$ is shown in Fig. 2.

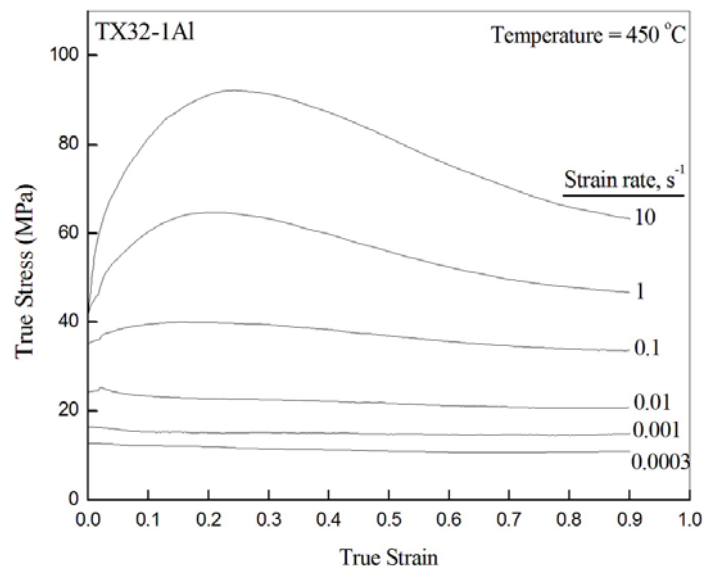


Fig. 2. True stress - true strain curves obtained on TXA321 alloy in compression at different strain rates for the test temperature of 450 $^{\circ}\text{C}$.

At strain rates lower to 1 s^{-1} , the flow curves exhibited near-steady state deformation. However, the specimens subjected to the high strain rates (10 and 1 s^{-1}) show the characteristic of flow softening. The occurrence of flow softening is an indication of either dynamic recrystallization (DRX) or flow instability and it is distinguished through further analysis of temperature and strain rate dependence of flow stress described below.

3.3 Processing Map

The processing map of as-cast TXA321 alloy obtained at a strain of 0.5 (steady state) is shown in Fig. 3. The map exhibits four domains in the temperature and strain rate ranges given as follows:

- (i) $300\text{-}325 \text{ }^\circ\text{C}$ and $0.0003\text{-}0.001 \text{ s}^{-1}$ with a peak efficiency of 31% occurring at $300 \text{ }^\circ\text{C}$ and 0.0003 s^{-1} (Domain # 1)
- (ii) $330\text{-}430 \text{ }^\circ\text{C}$ and $0.001\text{-}0.04 \text{ s}^{-1}$ with a peak efficiency of 33% occurring at $400 \text{ }^\circ\text{C}$ and 0.01 s^{-1} (Domain # 2).
- (iii) $430\text{-}500 \text{ }^\circ\text{C}$ and $0.01\text{-}0.5 \text{ s}^{-1}$ with a peak efficiency of 41% occurring at $500 \text{ }^\circ\text{C}$ and 0.1 s^{-1} (Domain # 3).
- (iv) $430\text{-}500 \text{ }^\circ\text{C}$ and $0.0003\text{-}0.002 \text{ s}^{-1}$ with a peak efficiency of 44% occurring at $475 \text{ }^\circ\text{C}$ and 0.0003 s^{-1} (Domain # 4).

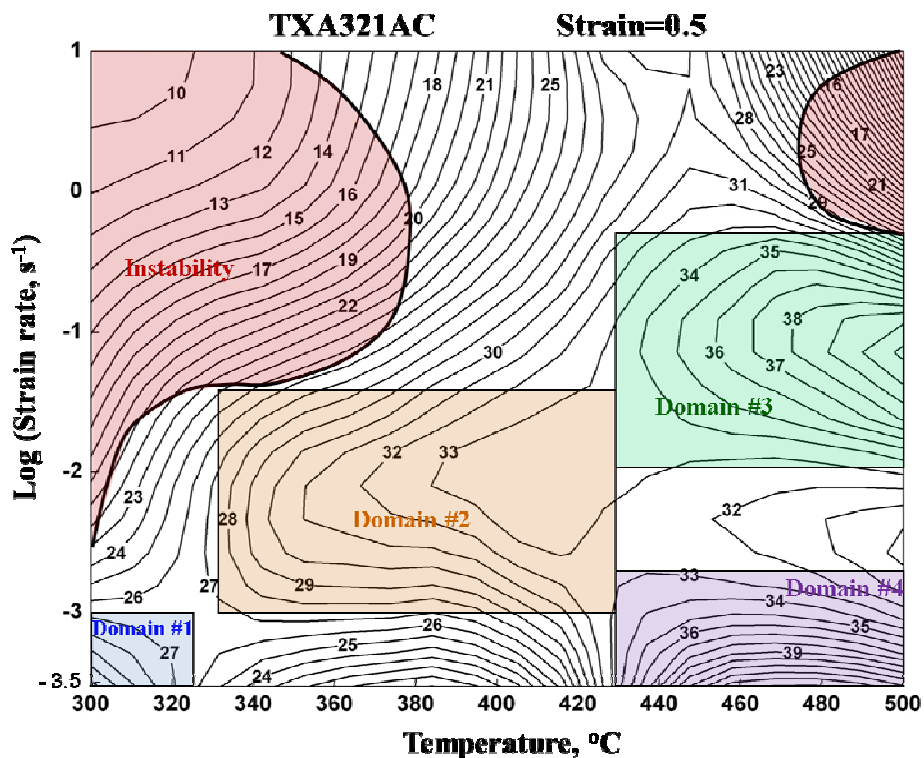


Fig. 3. Processing map for Mg-3Sn-2Ca-1Al (TXA321) alloy.

The map also exhibited two regimes of flow instability at (1) marked curved region occurred at lower temperature ($300\text{-}380 \text{ }^\circ\text{C}$) with high strain rates ($0.01\text{-}10 \text{ s}^{-1}$) and (2) higher temperature ($470\text{-}500 \text{ }^\circ\text{C}$) and at high strain rates (0.5 and 10 s^{-1}). The

microstructure obtained on specimen deformed under condition of peak efficiency in Domain #1 ($300\text{ }^{\circ}\text{C}/0.0003\text{ s}^{-1}$) is shown in Fig. 4(a) which exhibited fine, partially recrystallized grains indicating that DRX occurred in this domain. Fig. 4(b) shows the microstructure obtained on specimen deformed at peak efficiency condition in Domain #2 ($400\text{ }^{\circ}\text{C}/0.1\text{ s}^{-1}$) which shows that occurrence of DRX is higher compared to Domain #1. The microstructures from high temperature domains (#3 and #4) are also shown in Fig. 4(c-d) and reveals that complete DRX occurred in these domains as cast microstructure is completely converted into wrought microstructure.

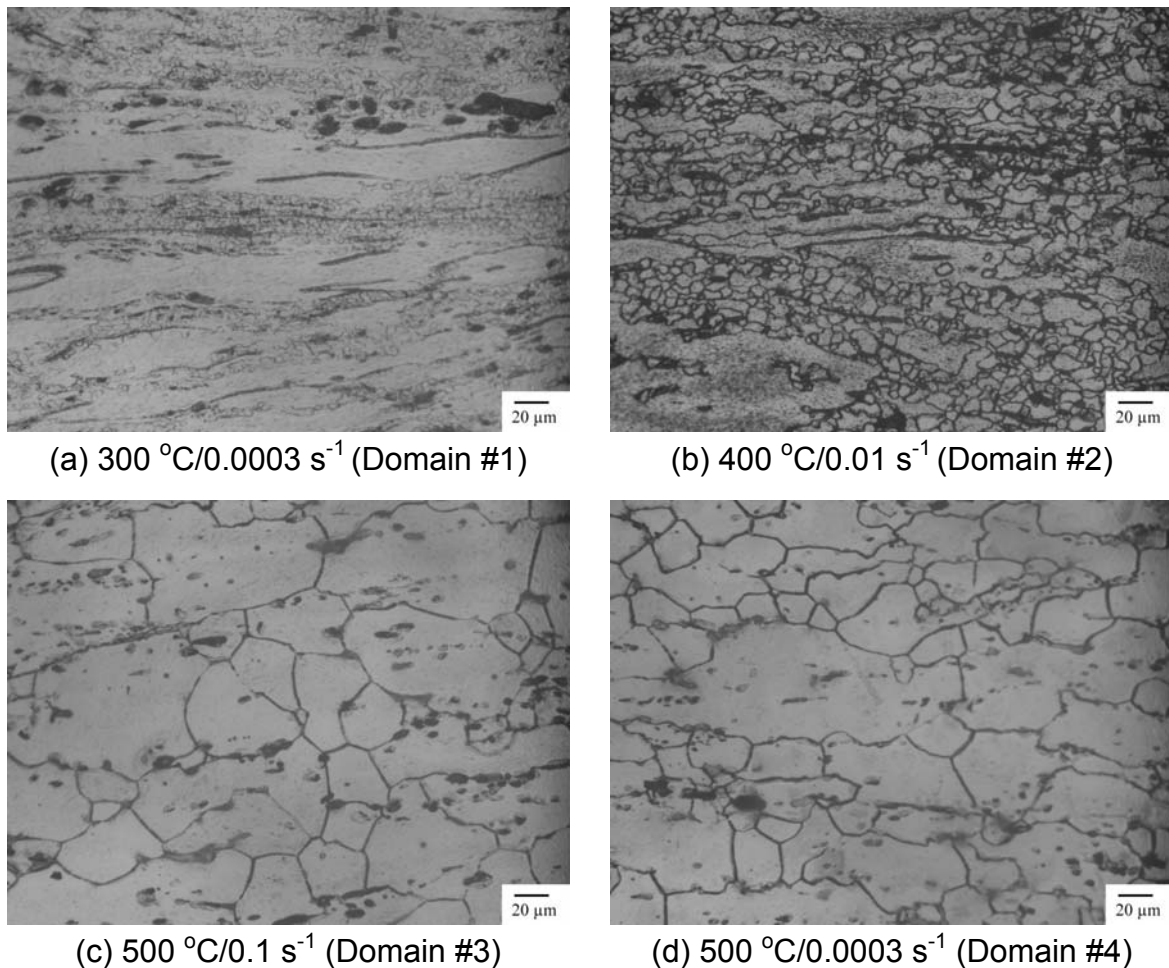


Fig. 4. Microstructures of TXA321 alloy representing various deformed conditions from the Domains. Compression axis is vertical.

3.4 Texture Evolution

Fig. 5(a) shows the pole figures of different reflections obtained on a specimen deformed at $300\text{ }^{\circ}\text{C}/0.0003\text{ s}^{-1}$ which correspond to the peak efficiency in the domain #1. The maximum intensity of basal poles is located at about $10\text{-}15^{\circ}$ with respect to the compression axis and formed basal textures. Prismatic poles are aligned normal to the compression axis making it unfavorable for the occurrence of prismatic slip. With the increase in temperature and strain rates i.e. at Domain #2 conditions (Fig. 5(b-c)), basal

poles are split and the deformation progressed due to the contribution of prismatic slip also and was evident from the Schmid factor plot shown in Fig. 6.

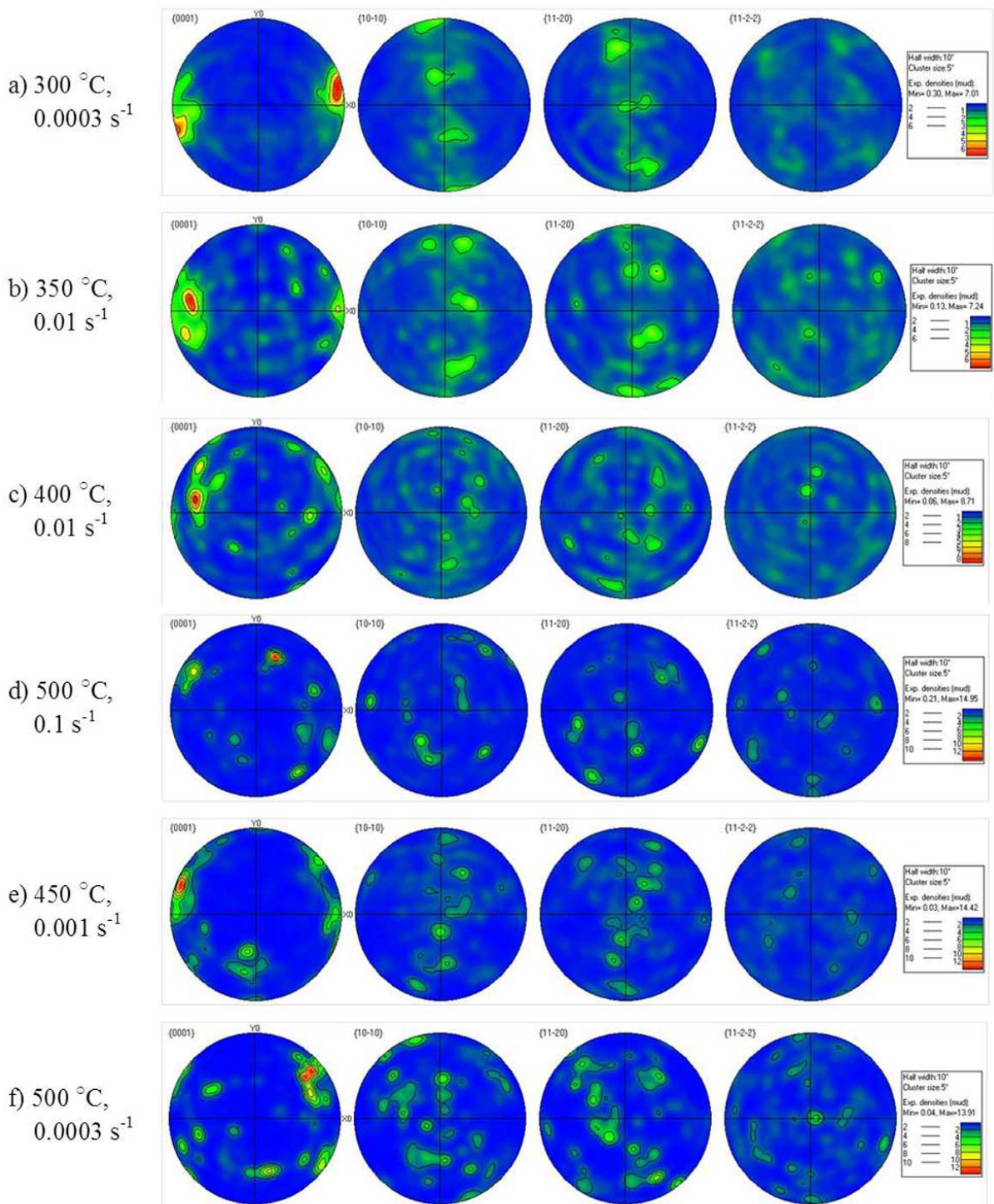


Fig. 5. Crystallographic textures using EBSD for various conditions (a) Domain #1, (b-c) Domain #2, (d) Domain #3, and (e-f) Domain #4. X-axis in pole figures is compression axis.

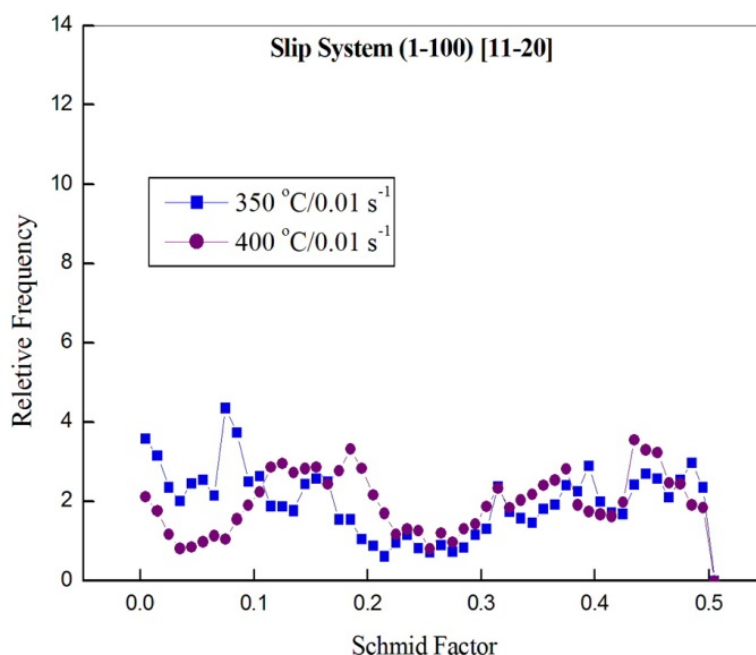


Fig. 6. Schmid factor distribution of the grains for prismatic slip system for the specimens deformed at 350 °C/0.01 s⁻¹ and 400 °C/0.01 s⁻¹ (Domain #2).

The pole figures obtained on the specimen deformed at 500 °C/0.1 s⁻¹ (peak efficiency condition from Domain #3) is shown in Fig. 5(d), all of which show that the texture is nearly random unlike the textures in the specimens deformed in domains #1 and 2. Deformation in domain #3 has a high contribution from second order pyramidal slip since the temperature range of this domain is 450-500 °C. A large number of these slip systems are available to take part in the deformation and the simultaneous recovery occurs by cross-slip of screw dislocations. The resulting DRX will randomize the texture in this domain. Similar characteristics can be observed from the pole figures (Fig. 5(e-f)) for Domain #4 conditions for lower strain rates (0.0003 and 0.001 s⁻¹) at the same temperature range.

4 CONCLUSIONS

Hot deformation behavior, microstructure and texture evolution of Mg-3Sn-2Ca-1Al (TXA321 alloy) in as-cast condition has been studied using hot compression tests in the temperature range 300-500 °C and strain rate range 0.0003-10 s⁻¹. The following conclusions are drawn from the present study:

- (i) Stress-strain curves exhibited flow softening at higher strain rates (>1 s⁻¹) while near steady state flow has been observed at lower strain rates at 450 °C.
- (ii) The processing map exhibits four domains of dynamic recrystallization at various temperature and strain rate range conditions. Map also shows two regimes of flow instability.
- (iii) Texture evolution as characterized by EBSD analysis revealed that in specimens deformed under conditions in domain #1 exhibited a basal texture with maximum intensity of basal poles is locating at about 10-15° to the compression direction.

- (iv) The basal poles are split and prismatic slip assisted for deformation in Domain #2.
- (v) At temperatures 450 and 500 °C (domains #3 and #4), second order pyramidal slip activity has significantly increased along with cross-slip which randomized the texture under conditions of peak efficiency in these domains (500 °C/0.1 s⁻¹ and 500 °C/0.0003 s⁻¹).

ACKNOWLEDGEMENT

This work was supported by General Research Funding (Project #115108) from the Research Grants Council of the Hong Kong Special Administrative Region, China.

REFERENCES

- Abu Leil, T et al., (2006), "Corrosion behavior and microstructure of a broad Range of Mg-Sn-X alloys", *Magnesium Technology 2006*, Warrendale, PA, pp. 281-286.
- Abu Leil, T et al., (2007), "Microstructure, Corrosion and Creep of as-cast Magnesium alloys Mg-2Sn-2Ca and Mg-4Sn-2Ca", *Magnesium Technology 2007*, Warrendale, PA, pp. 257-262.
- Frost, H.J. and Ashby, M.F. (1982), *Deformation-Mechanism Maps: The plasticity and Creep of Metals and Ceramics*, Pergamon Press, Oxford, p. 44.
- Hosford, W. (1993), *The Mechanics of Crystals and Textured Polycrystals*, New York: Oxford University Press, USA, 122-124.
- Kozlov, A. Ohno, M. Arroyave, R. Liu, Z.K. and Schmid-Fetzer, R. (2008), "Phase equilibria, thermodynamics and solidification microstructures of Mg-Sn-Ca alloys, Part 1: Experimental investigation and thermodynamic modeling of the ternary Mg-Sn-Ca system", *Intermetallics*, Vol. **16**, 299-315.
- Prasad, Y.V.R.K. Gegel, H.L. Doraivelu, S.M. Malas, J.C. Morgan, J.T. Lark, K.A. Barker, D.R. (1984), "Modeling of dynamic material behavior in hot deformation: Forging of Ti-6242" *Metall. Trans.* Vol. **15A**, 1883-1892.
- Prasad, Y.V.R.K. and Seshacharyulu, T. (1998), "Modeling of hot deformation for microstructural control", *Inter. Mater. Rev.* Vol. **43**, 243-258.
- Prasad, Y.V.R.K. (2003), "Processing maps: A status report", *Jour. Mater. Eng. Perf.* Vol. **12**, 638-645.
- Prasad, Y.V.R.K. and Rao, K.P. (2008), "Processing maps for hot deformation of rolled AZ31 magnesium alloy plate: Anisotropy of hot workability", *Mater. Sci. Eng. A*, Vol. **487**, 316-327.
- Rao, K.P. Prasad, Y.V.R.K. Hort, N. Huang. Y. and Kainer K.U. (2007), "High temperature deformation of a new magnesium alloy", *Key Eng. Mater.*, Vol. **340-341**, 89-94.